IDENTIFICATION OF LAND-COVER FEATURES'S PHENOLOGY USING MULTITEMPORAL SENTINEL-1 DATA: A CASE STUDY IN HANOI, VIETNAM

Hang Le Minh[1], Truong Vu Van[1], Duong Nguyen Dinh[2] and Tuan Tran Anh[3]
[1] Le Quy Don Technical University, 236 Hoang Quoc Viet street, Cau Giay, Hanoi, Vietnam
Email: leminhhang81@gmail.com, truongvv@mta.edu.vn
[2] Institute of Geography, Vietnam Academy of Science and Technology, Hanoi, Vietnam,
Email: duong.nguyen2007@gmail.com
[3] Institute of Ecology and Biological Resources, Vietnam Academy of Science and Technology, Hanoi, Vietnam
Email: tuan.ig@gmail.com

KEY WORDS: SAR, phenology, land cover, multi-temporal, Sentinel-1

ABSTRACT: Hanoi regions are experiencing rapid land cover changes caused by human-included land degradation and extreme climates events. Identification the changes in vegetation phenology and in land-cover play an integral part for management and urban planning. Multi-temporal satellite image data are accepted as being the best material to map these changes, especially SAR images. SAR images are unaffected by weather conditions, clouds and operating all day and night. Currently, the Sentinel-1 data of European Space Agency (ESA) are free. The Sentinel-1A satellite carries a C-band Synthetic Aperture Radar, spatial resolution is 10 meters and acquisition cycle is 12 days. In the article, the authors present the correlation between the change of rice phenology and backscatter value on multi-temporal Sentinel-1 images. At the same time, the authors also propose a method of determining land-cover objects of Hanoi Vietnam on multi-temporal SAR images base on integrating changed/unchanged objects, mean backscattering value and rice phenology. The accuracy achieved 89.6%.

1. INTRODUCTION

Land-cover (*i.e*, biophysical attributes of the Earth's surface) and land-use (human purpose applied to these attributes) changes are among the most important drivers of the Earth's global change [10], [13]. Land-cover changes may result from human included land-use changes or natural processes such as climatic variability and natural disturbances [1]. The status and rate of land-cover changes may be estimated through a monitoring approach with remotely sensed data [9]. In recent years, land-cover classification methods commonly used optical satellite image data based on spectral characteristics of the objects [1], [2]. However, the disadvantages of optical satellites are influenced by climatic conditions. Therefore, it is very difficult to collect optical images in northern Vietnam because of clouds. Microwave remote sensing satellite is suitable for Vietnam. The advantages of SAR images are unaffected climate condition, all day and night. The backscatter in SAR image is affected by roughness, conductivity, polarization of the signal. So that it is difficult to classify land-cover by only one SAR image. Land-cover may be classified by multi-temporal SAR images [14], [5].

Beside that, the changes of vegetation, specially cropland, affect to the change of the others land-cover objects. Changes of vegetation have been using to derive a measure that correlates with surface biophysical properties [11] that facilitate the analysis of large amounts of satellite data by providing valuable large spatial- and temporal-scale analyses [14]. These changes have contributed to characterize seasonal variations and phenology activity of vegetation in time series of satellite data, providing baseline data to monitor length of the growing season, peak greenness, onset of greenness, or land-cover changes associated with events such as fire, drought, land-use conversion, and climate fluctuation [1], [12], [6]. Recently, multiple studies presented to identify vegetation phenology and land-cover objects by multi-temporal SAR images data such as ALOS PALSAR, EnviSAT ASAR, Radarsat, Terra-X [14],[16], [5]… In these research the major classification method is used by decision tree [5], [5].

The SENTINEL-1 mission is the European Radar Observatory for the Copernicus joint initiative of the European Commission (EC) and the European Space Agency (ESA). Copernicus, previously known as GMES, is a European initiative for the implementation of information services dealing with environment and security. It is based on observation data received from Earth Observation satellites and ground-based information. The SENTINEL-1 mission includes C-band imaging operating in four exclusive imaging modes with different resolution (down to 5 m) and coverage (up to 400 km). It provides dual polarization capability, very short revisit times and rapid product delivery. For each observation, precise measurements of spacecraft position and attitude are available. Sentinel-1A is a European radar imaging satellite launched in 2014. Sentinel-1 data is offered free. And this is a new SAR data on Earth Observation mission [17].

In this article, the authors present the experimental results of Sentinel-1 data. In which we assess the stability of the backscatter values on the time-series Sentinel-1 images. Also, the authors propose a land-cover classification method on multi-temporal Sentinel-1 images by combining difference result images, such as the standard deviation backscatter image, the mean backscatter value image and the rice phenology image.

2. STUDY AREA AND DATA PROCESSING

2.1. STUDY AREA AND DATA PRE-PROCESSING

Hanoi is located between 20°53' to 21°23' north latitude and 105°44' to 106°02' east longitude, adjacent to Thai Nguyen province, Vinh Phuc province in the North; Ha Nam province and Hoa Binh in the South; Bac Giang province, Bac Ninh province and Hung Yen province in the East; and Hoa Binh province and Phu Tho province in the West. The Red River is a main river of Hanoi. Its section flowing through Hanoi from Dong Anh district to Thanh Tri district is 40 km long. The Duong the second largest river in Hanoi separates itself from the Red River at Xuan Canh (Xuan Canh commune, Dong Anh). Besides these two rivers, Hanoi has many other waterways, which, although smaller and shorter, are connected with the long-standing history of Hanoi, for instance, the To Lich River.

The majority of the Ha Noi area is situated in the Viet Nam's Red River delta with an average elevation of 5m to 20m above sea level. The hilly areas are in the north and northwest of Soc Son district of the southern edge of Tam Dao Mountains with elevations from 20m to over 400m. The highest peak is Chan Chim peak at 462 m. The topography of Ha Noi decreases height from north to south and from west to east. The main topographic form is the high alluvial terraces interspersed with low lying lakes. The high terraces are only in Soc Son district in northern and eastern of Dong Anh district. In addition are mountainous terrain and hills concentrated in Soc Son mountain area.

The Hanoi climate is typical for a tropical monsoon climate of the northern climate (hot in the summer, rainy and cold winter, less rainy). With location among tropical zone, Hanoi gets abundant of solar radiation and high temperatures around the year. The amount of total radiation average s 11,8 kcal/cm^2 and year average temperature is 23,6°C. Due to the influence of the East Sea, Hanoi temperature is quite high humidity and rainfall. The average annual humidity is around 79% a year and rainfall is 1,800 mm. There are approximately 114 days raining a year here.

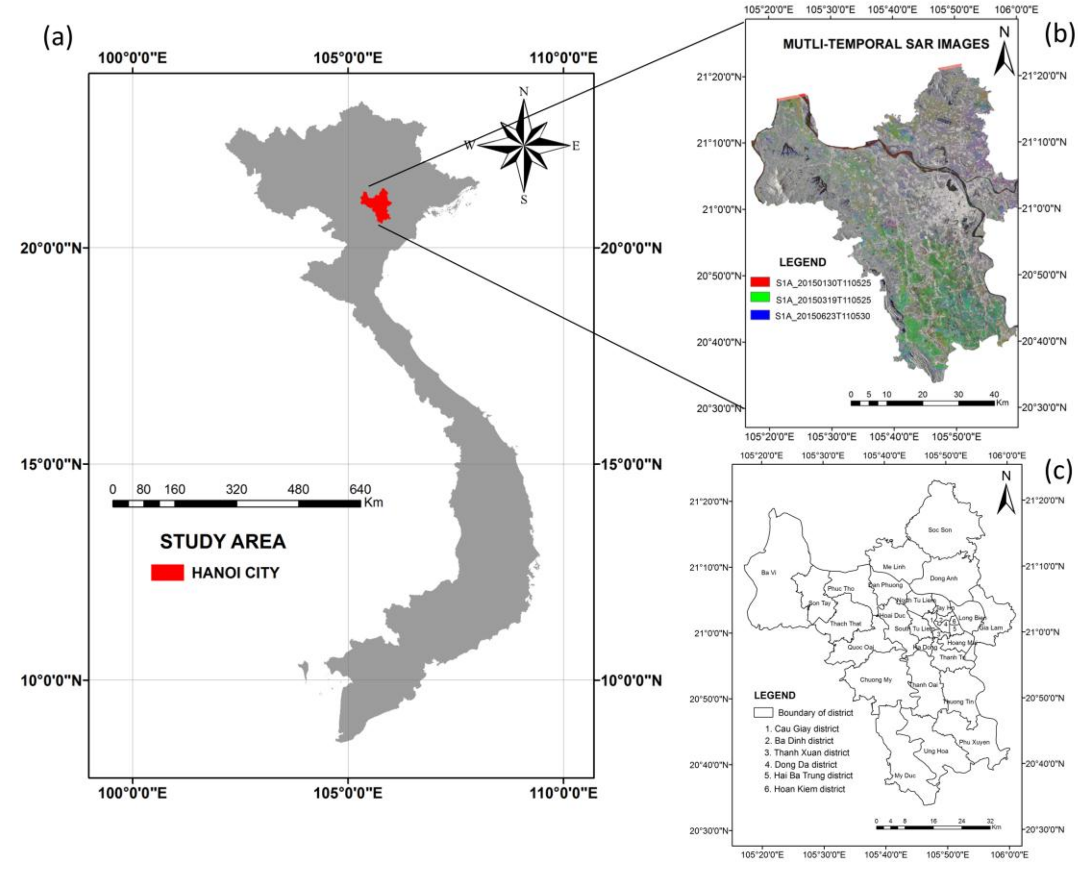

Figure 1. (a) Location of Hanoi in Vietnam; (b) The RGB composite image of three-times Sentinel-1 images; (c) Boundary of districts in Hanoi

The main land-cover objects of Hanoi included in developed land, barren land , water , Wetlands , forest, cropland . In recent years , Hanoi has a rapid urbanization rate , around 3.5 % a year. The increasingly urbanization has changed the annual land-cover objects, especially developed land and crop-land. The area of cultivated land is decreased. The cultivated land of rice is changed to barren land. Therefore, updated real-time the changes of land-cover by the multi-temporal microwave image data is important to give development policies of Hanoi .

2.2. Data material and pre-processing

2.2.1. Data material

Sentinel-1 is a two satellite constellation with the prime objectives of Land and Ocean monitoring. The Sentinel-1A was launched on 03 April 2014. The goal of the mission is to provide C-Band SAR data continuity following the retirement of ERS-2 and the end of the EnviSAT mission. To accomplish this the satellites carry a C-SAR sensor, which offers medium and high resolution imaging in all weather conditions. The C-SAR is capable of obtaining night imagery and detecting small movement on the ground, which makes it useful for land and sea monitoring. It had a 12 day repeat cycle and was operated by the European Space Agency (ESA). Multiple orbit paths can be used to observe the same area in a shorter time due to the side-looking nature of the C-SAR sensor with different incidence angles ranging from 29.1° to 46.0° (Interferometry Wide Swath).

For this study, we had access to almost all archived Interferometry Wide Swath mode acquisition from December 2014 through October 2015 that completely cover the Hanoi area. Interferometry Wide Swath data is acquired in three swaths using the Terrain Observation with Progressive Scanning SAR (TOPSAR) imaging technique. IW is SENTINEL-1's primary operational mode over land. A total of 10 Sentinel-1 IW VV polarization images at 10m spatial resolution with 250 km swath width. We used Level-1 Ground Range Detected (GRD) products. This level consist of focused SAR data that has been detected, multi-looked and projected to ground range using an Earth ellipsoid model such as WGS84. The ellipsoid projection of the GRD products is corrected using the terrain height specified in the product general annotation. The terrain height used varies in azimuth but is constant in range [17]. Details of the characteristics of the Sentinel-1 data used in this study are shown in **Table 1**.

Table 1. Multi-temporal Sentinel-1 experiment data

No	Acquisition date	Orbit	Pixel spacing (m)	Polarization
1	13/12/2014	Ascending	10x10m	VV
2	06/01/2015	Ascending	10x10m	VV
3	23/02/2015	Ascending	10x10m	VV
4	19/03/2015	Ascending	10x10m	VV
5	12/04/2015	Ascending	10x10m	VV
6	30/05/2015	Ascending	10x10m	VV
7	23/06/2015	Ascending	10x10m	VV
8	17/07/2015	Ascending	10x10m	VV
9	03/09/2015	Ascending	10x10m	VV
10	21/10/2015	Ascending	10x10m	VV

2.2.2. Data pre-processing

All Sentinel-1 data were pre-processed using the open source software SNAP Toolbox of European Space Agency. Pre-processing of SAR image consisted of geocoding, radiometric calibration, incidence angle normalization. The geocoding step involved a Range Doppler Terrain correction processing that used the elevation data from the 3 arc-second DEM product from the Shuttle Radar Topography Mission (SRTM) provided by ESA. In this process, data are resampled and geo-coded to a grid of 10m spacing to preserve the 20mx5m spatial resolution according to the NY Quist sampling thermo. The data pre-processing in this study has been performed in three main steps such as (1) Resampled and geo-coded by DEM product; (2) Backscatter normalization to sigma-nought (σ^0) of intensity band; (3) Convert linear to/from dB.

In the second step, the following parameters obtained for each scene is sigma-nought backscatter coefficient (σ^0). According to the theory, the backscatter is not only influenced by the characteristic of land cover but also the incidence angle. In order to detect changes in backscatter resulting from a change in surface status or land cover, it is necessary to remove incidence angle dependency of backscatter by normalizing all acquisition to a common incidence angle. This was achieved by the approach described in Daniel Sabel's paper [4]. In this SNAP toolbox, the objective of SAR calibration output scaling applied by the processor must be undone and the desired scaling must be applied. Level-1 products provide four calibration Look Up Tables (LUTs) to produce σ^0 . The LUTs apply a range-dependent gain including the absolute calibration constant. For GRD products, a constant offset is also applied. The radiometric calibration is applied by the following Eq (1):

$$\sigma_i^0 = \frac{|DN_i|^2}{A_i^2} \quad (1)$$

Where, DN_i depending on the selected LUT, A_i - beta-nought (i). Bi-linear interpolation is used for any pixels that fall between points in the LUTs

After that backscatter normalization to sigma-nought, we used Convert linear to dB module of SNAP toolbox to convert value to decibels. The backscatter cross section of converted image is illustrated in Figure 2.

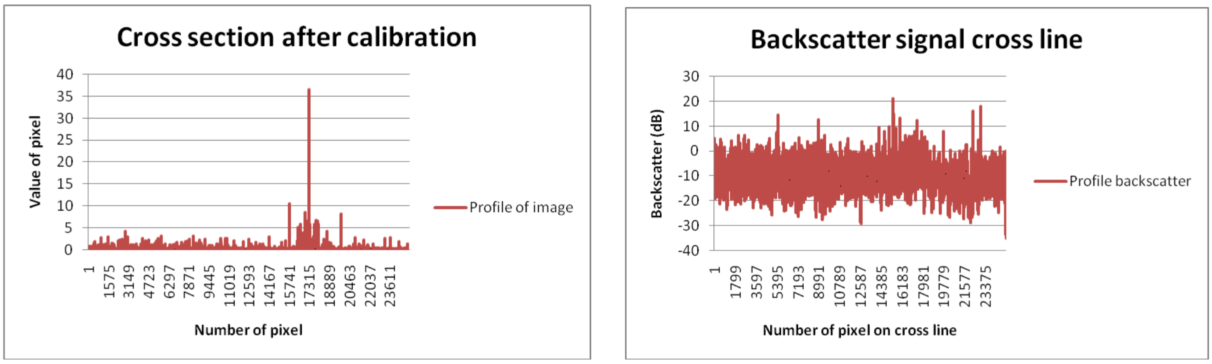

(a) (b)

Figure 2. (a) Cross section of image after calibration; (b) Backscatter cross section after conversion to dB

In Figure 2, the backscatter signal in near-range was the same far-range in a cross section. As a result the converted image was normalized incidence angle.

Beside that, the stability of the image backscatter values of time-series SAR image after sigma-nought normalization is need for studying in classification the land-cover by multi-temporal images. We presented the analysis result of backscatter included of maximum value, minimum value, average value and standard deviation of Sentinel-1 time-series at the same area of Hanoi. The analytical results are shown in Figure 3.

	Min	Max	Mean	Stdev
13-Dec-14	-31.650	34.861	-4.491	5.586
6-Jan-15	-29.671	35.580	-4.787	5.958
23-Feb-15	-31.517	34.747	-4.789	5.964
19-Mar-15	-29.661	36.022	-3.941	4.988
12-Apr-15	-31.021	35.855	-3.862	4.967
30-May-15	-30.287	35.424	-3.873	5.015
23-Jun-15	-30.851	35.844	-4.278	5.547
17-Jul-15	-30.371	36.358	-3.897	4.998
3-Sep-15	-30.839	35.353	-3.763	4.976
21-Oct-15	-30.530	35.259	-3.814	4.970
13-Dec-14	-31.650	34.861	-4.491	5.586

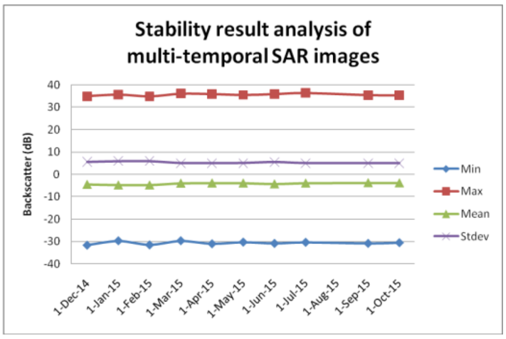

Figure 3. Analysis stability of backscatter value of multi-temporal SAR images

In Figure 3, we can see the stability of backscatter value of multi-temporal Sentinel-1 images after pre-processing. It proves that the pre-processing Sentinel-1 by 3 steps ensure to compare of backscatter value of the object land-cover on multi-temporal images.

2.2.3. Field Survey data

A field survey was conducted by using the Locus map which is an application software on Android system. Locus map is capable of locating points by GPS and taking photos. A distance of 40 km was covered the study area during the survey and around 100 ground truth points were collected. The ground truth points include the change/unchange land cover classes, crop land and rice fields.

3. METHODOLOGY

3.1. Changed/Unchaged objects

Considering in period of one year, the land cover objects on SAR image are divided into two main groups:

+ Changed Objects (Objects fluctuate over time)

+ Unchanged objects (Objects do not fluctuate or hardly changes over time)

Unchanged objects are objects such as developed land, forestry land, water, barren land. Backscattering of water vary due to the movement of vehicles on the water surface, which creates changes the surface at the time signals are being received. Forestry land which include trees in a forest, trees in urban and fruit trees ... are not the kind of deciduous trees. Forestry land in Hanoi are mainly evergreen forest, canopy density therefore unchanged over time.

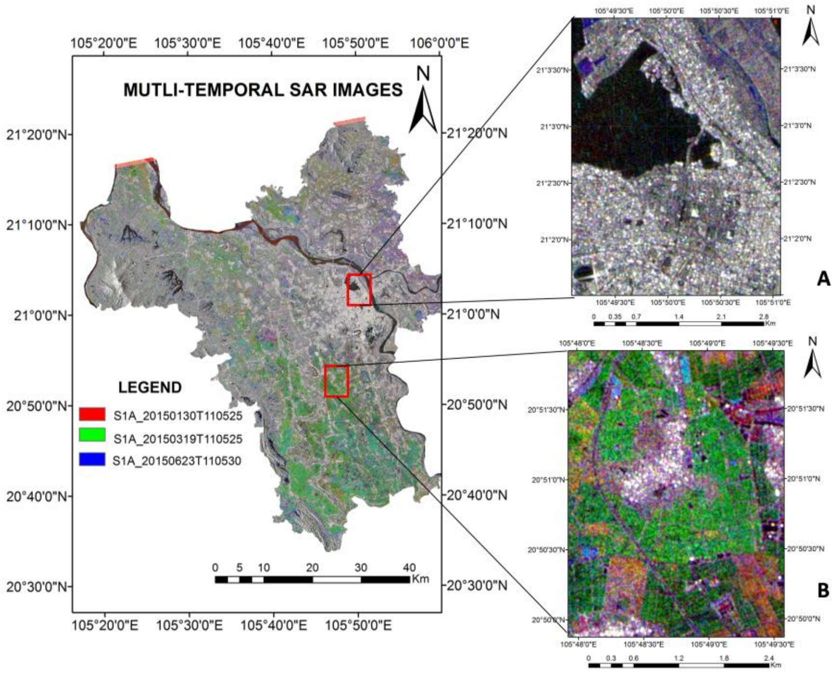

Figure 4. (a) The unchanged area on the RGB composite image of three-times Sentinel-1 images; (b) The changed area on The RGB composite image of three-times Sentinel-1 images

The results of analysis backscatter values of land-cover objects on multi-temporal Sentinel-1 images are shown on Figure 5.

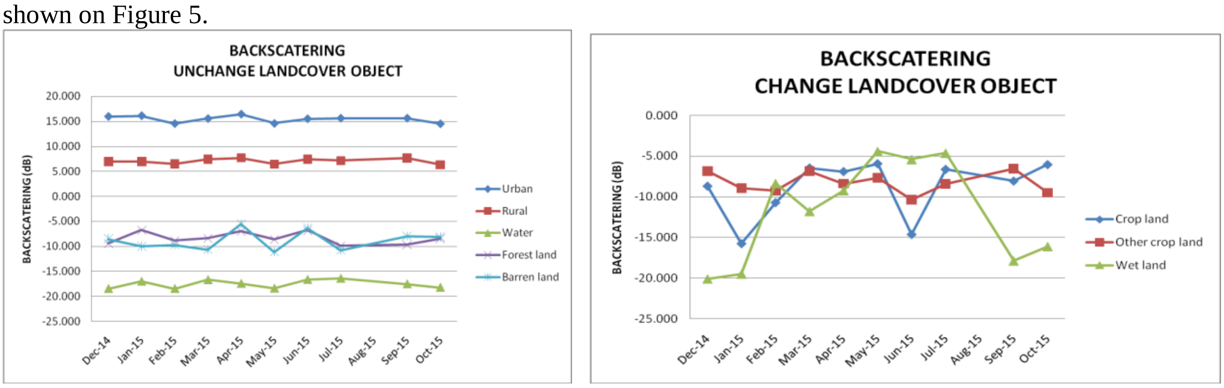

(a) (b)

Figure 5. (a) Backscatter (dB) of land-cover unchanged objects; (b) Backscatter (dB) of land-cover changed objects

Figure 5a shows the backscattering values of developed land objects. In the urban areas, they have the highest backscattering, in the range of +15dB and +20dB. Whereas the backscattering of these objects , in rural areas, are lower, ranging from + 10dB to + 5dB. Forestry land has the backscattering ranges from -10dB to -5dB. backscattering of barren land similar to values of forest (-12dB to -5 dB). Meanwhile, water has the lowest backscattering, ranging from -20dB to -15dB.

(a) (b)

Figure 6. (a) Field surveying photo of wetland; (b) Field surveying photo of deciduous tree

3.2. Phenology of rice

In theory, the variation of the value of backscattering on SAR images will depend on the change of the objects. Here, rice is cultivated seasonally so backscattering values on SAR images will depend on the growth of rice (Figure 7).

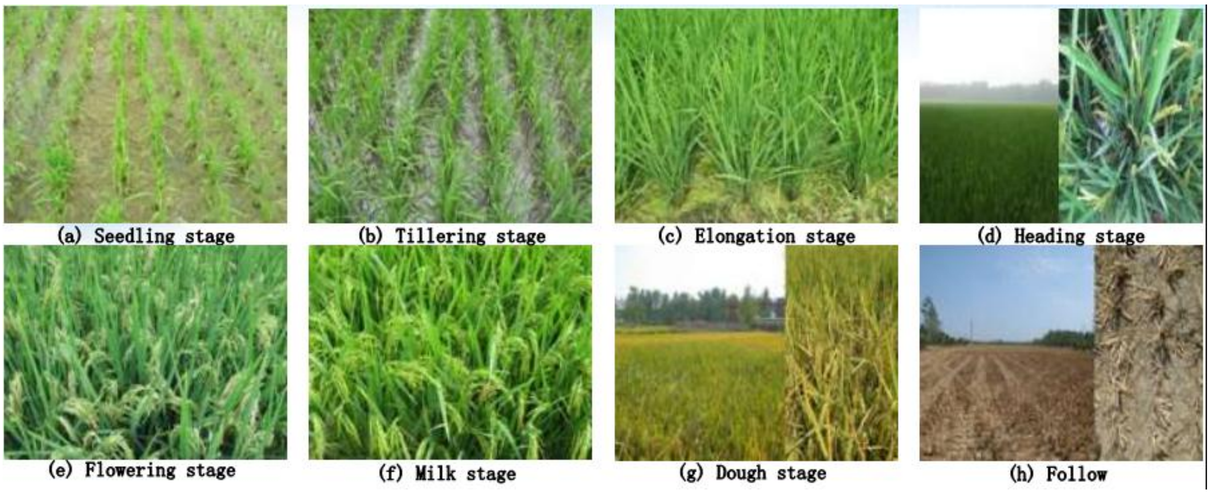

Figure 7. **Rice phenology (Hybrid rice)**

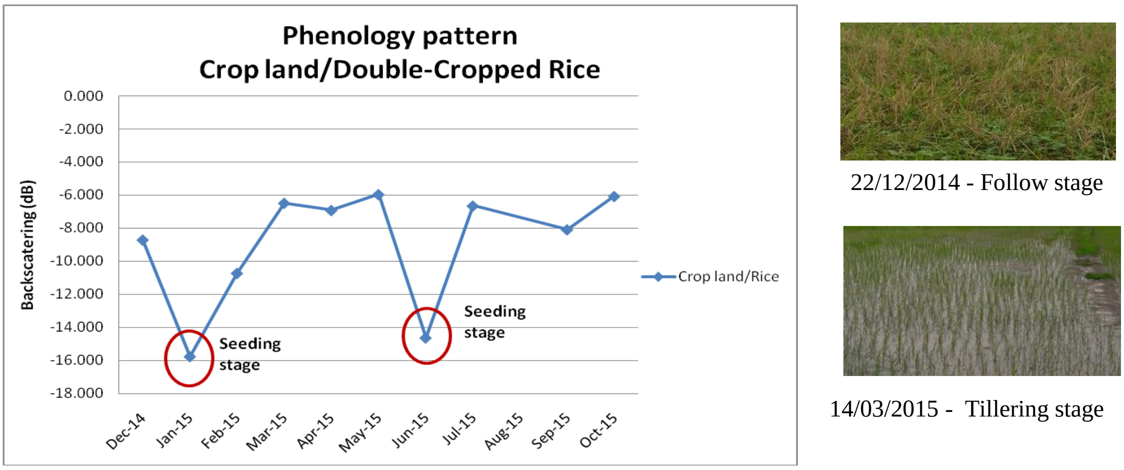

Figure 8. Phenology pattern Crop land/Double-Cropped Rice in Sentinel-1 data

According to a field survey in the growing rice area of Hanoi, the lands are mainly used for growing rice from January to June and from July to October. In the others period, these lands were abandoned or used for growing crops, due to rice cultivation in this period did not bring high economic efficiency. There are big changes with wetland objects in the western region of Hanoi due to the water surface areas are used for farming or other purposes (Figure 5b and Figure 8).

3.3. Proposal method

In this study, the authors proposed a classification method for land cover objects using multi-temporal Sentinel-1 images. This method based on the characteristics: changed or unchanged of the objects. The unchanged land cover objects in Hanoi including developed land, water and evergreen forests. The changed objects are seasonal crops such as rice, maize and other crops objects. The main food crops, in Hanoi, always be paddy therefore with changed objects, to classify rice objects, the authors will be based on phenology of crops on multi-temporal SAR images. As for other changed subjects, such as corn and other crops, will be assigned by a other crop land layer because of their small and not fixed cultivation area.

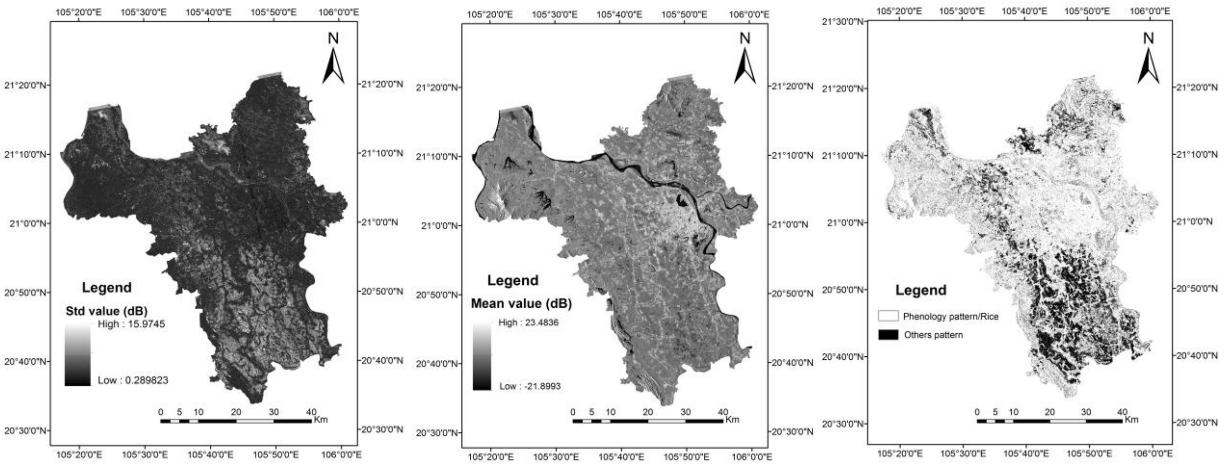

(a) (b) (c)

Figure 9. (a) Standard deviation image; (b) the mean value image; (c) The phenology cropland image

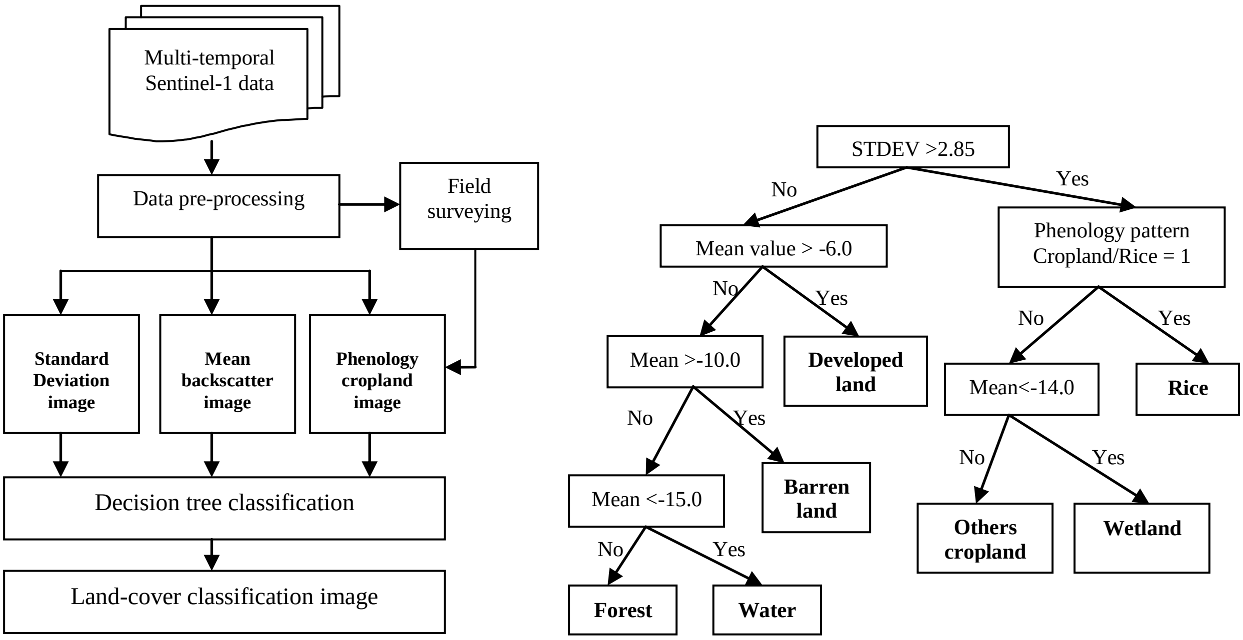

(a) (b)

Figure 10. (a) The flowchart of proposal classification method; (b) The threshold of decision tree classification

To evaluate the changes of the land cover objects in one-year cycle, the authors based on the standard deviation value of backscattering value on multi-temporal Sentinel-1 images. This standard deviation value is determined by Eq (2):

$$std = \left(\frac{1}{n-1} \sum_{i=1}^{n} \left(x_i - \bar{x} \right)^2 \right)^{\frac{1}{2}} \quad (2)$$

where $\bar{x} = \frac{1}{n}\sum_{i=1}^{n} x_i$ is the average backscatter value of multi-temporal pixel; x_i is backscatter value of each pixel at period image

In Figure 5a, there are some difference mean backscatter value between the changed objects including urban, rural, water, forest, barren-land. Developed land objects (both of urban and rural) have high backscatter values; water objects have low values; both of barren-land objects and evergreen forest objects have medium backscatter value. Among the changed objects, rice changes seasonally. Based on the phenology of the rice in multi-temporal image and cultivation conditions (weather and soil type) in Hanoi, the authors calculated phenology pattern cropland image. Low peak values of rice on the phenology graph of rice are backscattering values in January and July (Figure 8).

After determining the intermediate images including Standard deviation image, mean value image, phenology cropland/Rice image (Figure 9) by Matlab 2014a software, the authors use a decision tree method to establish the land cover classification map on multi-temporal Sentinel-1 image (Figure 11). The threshold values in the decision tree method are shown in Figure 10b.

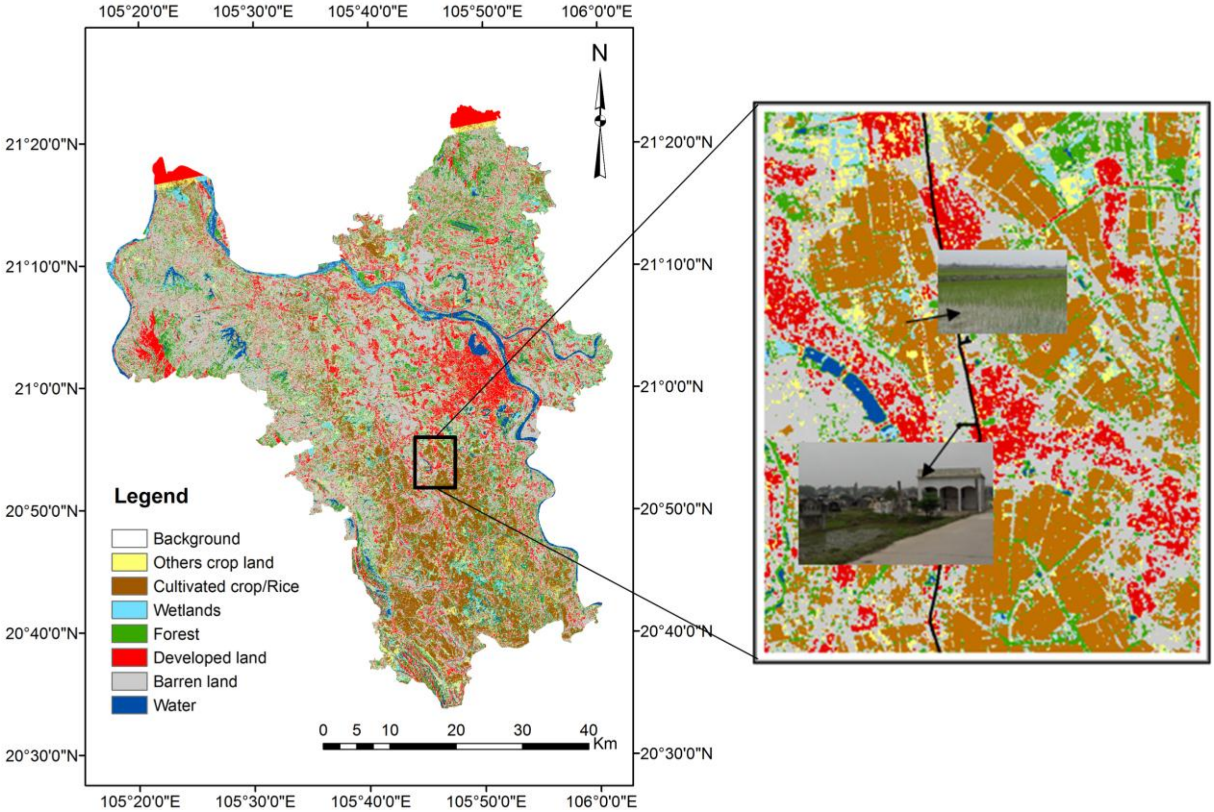

Figure 11. (a) Lancover classification map of Hanoi Vietnam; (b) Test result classification by field surveying

4. RESULT AND DISCUSSION

The land cover classification results on multi-temporal Sentinel-1 show in Figure 11a. To evaluate the accuracy of classification results, the authors conducted field checks. Fieldwork route is shown in Figure 11b. In addition, the accuracy of classification results is also determined by the creat random point modul in ArcGIS and checked on high resolution satellite images on Google Earth. Number of checkpoints are 100 points. The accuracy had 89.6%.

Experimental results show that the classification of developed land and rice objects has high accuracy. The method proposed in the paper still exists some disadvantages. The regions shadowed by the high mountain have a strong reflection intensity on SAR image, which caused misclassified (high mountainous areas into residential areas with high density). In addition, due to the change of water level leading to the wetland objects are still mixed with water objects.

5. CONCLUSION

The decision tree classification method on multi-temporal SAR image have been many scientists mentioned with many different purposes, especially in land cover classification and in determining phenology of rice and crops such as corn and wheat.... The proposed method in the paper based on the changes/unchanges backscatter value and phenology cropland with the results achieved 89.6%. These are results of research carried out on the Sentinel-1 material and have been tested by field surveying data therefore this research has high reliability. Thus it can be concluded that the land cover classification can be resolved on the multi-temporal Sentinel-1 (with IW mode and single-polarization VV) image. In subsequent studies, the authors will focus on the study of crops phenology such as corn, seasonal crops, deciduous trees, evergreen forests ... to be able to extract more information on the image. At the same time, we will combine with the data which are classified on Landsat 8 to enhance the ability to automatically and accurately determine the land cover on the whole territory of Vietnam.

ACKNOWLEDGE

This research is funded by Vietnam National Foundation for Science and Technology Development (NAFOSTED) under grant number 105.08-2014.14.

REFERENCES

1. Abdalla M. Faid & Abdulaziz M. Abdulaziz, 2012. Monitoring land-use change-associated land development using multitemporal Landsat data and geoinformatics in Kom Ombo area, South Egypt, *International Journal of Remote Sensing*, Vol. 33, No. 22, 20 November 2012, 7024–7046.
2. BjörnWaske, Matthias Braunb, 2009. Classifier ensembles for land cover mapping using multitemporal SAR imagery. ISPRS Journal of Photogrammetry and Remote Sensing 64 (2009) 450-457.
3. Duong Nguyen Dinh, Anh Le Van, Thu Ho Le, 2014. Interpretation of land cover using spectral modulation pattern an example with Landsat 8 OLI image, *Vietnam Journal of Earth Sciences*, Vol.36 (2014), pp 480-488.
4. Daniel Sabel, Zoltan Bartalis, Wolfgang Wagner, Marcela Doubkova, Jean-Pierre Klein, 2012. Development of a Global Backscatter Model in support to the Sentinel-1 mission design. Remote Sensing of Environment 120 (2012), 102-112.
5. Duy Ba Nguyen, Kersten Clauss, Senmao Cao, Vahid Naeimi, Claudia Kuenzer and Wolfgang Wagner, 2015. Mapping Rice Seasonality in the Mekong Delta with Multi-Year Envisat ASAR WSM Data. Remote Sensing 2015,7, 15868-15893; doi:10.3390/rs71215808.
6. Justice, C.O.; Holben, B.N.; Gwynne, M.D. Monitoring East African vegetation using AVHRR data. Int. J. Remote Sens. 1986, 7, 1453-1474.
7. Huete, A.; Justice, C.; van Leeuwen, W. MODIS Vegetation Index (MOD 13). Algorithm Theoretical Basis Document, Version 3; NASA Goddard Space Flight Center: Greenbelt, MD, USA, 1999.
8. Lupo, F.; Linderman, M.; Vanacker, V.; Bartholomé, E.; Lambin, E.F. Categorization of land-cover change processes based on phenological indicators extracted from time series of vegetation index data. Int. J. Remote Sens. 2007, 28, 2469-2483.
9. Li, J.; Lewis, J.; Rowland, J.; Tappan, G.; Tieszen, L.L. Evaluation of land performance in Senegal using multi-temporal NDVI and rainfall series. J. Arid Environ. 2004, 59, 463-480.
10. Lambin, E.F.; Baulies, X.; Bockstael, N.; Fischer, G.; Krug, T.; Leemans, R.; Moran, E.F.; Rindfuss, R.R.; Sato, Y.; Skole, D.; Turner, B.L., II; Vogel, C. Land-Use and Land-Cover Change (LUCC) Implementation Strategy; IGBP Report No. 48/IHDP Report No 10; International Geosphere-Biosphere Programme (IGBP): Stockholm, Sweden, 1999.
11. Myneni, R.B.; Hall, F.G.; Sellers, P.J.; Marshak, A.L. The interpretation of spectral vegetation indexes. IEEE Trans. Geosci. Remote Sens. 1995, 33, 481-486.
12. Moody, A.; Johnson, D. Land-surface phenologies from AVHRR using the discrete Fourier transform. Remote Sens. Environ. 2001, 75, 305-323.
13. Richards, J.F. Land transformations. In The Earth as Transformed by Human Action: Global Change and Regional Changes in the Biosphere Over the Past 300 Years; Turner, B.L., II, Clark, W.C., Kates, R.W., Richards, J.F., Mathews, J.T., Meyer, W.B., Eds.; Cambridge University Press: New York, NY, USA, 1990.
14. Tucker, C.J.; Townshend, J.R.G.; Goff, T.E. African land-cover classification using satellite data. Science 1985, 227, 369-375.
15. Yuan Zhang , Cuizhen Wang , Jiaping Wu , Jiaguo Qi & William A. Salas, 2009, Mapping paddy rice with multitemporal ALOS/PALSAR imagery in southeast China, International Journal of Remote Sensing, Vol. 30, No. 23, 10 December 2009, 6301–6315
16. Zhiyuan Pei, Songling Zhang, Lin Guo, Heather McNairn, Jiali Shang & Xianfeng Jiao, 2011. Rice identification and change detection using TerraSAR-X data, Canadian Journal of Remote Sensing, Vol. 37, No. 1, pp. 151 156, 2011
17. https://earth.esa.int/web/sentinel/user-guides/sentinel-1-sar